



Atomistic study of two-dimensional discrete breathers in hcp titanium

O. V. Bachurina^{1,a} , R. T. Murzaev², A. A. Kudreyko³, S. V. Dmitriev^{1,4}, and D. V. Bachurin^{5,6}

¹ Ufa State Petroleum Technological University, Kosmonavtov St. 1, 450062 Ufa, Russia

² Institute for Metals Superplasticity Problems, Russian Academy of Sciences, Khalturin St. 39, 450001 Ufa, Russia

³ Bashkir State Medical University, Lenina St. 3, 450008 Ufa, Russia

⁴ Institute of Molecule and Crystal Physics, Ufa Federal Research Center of the Russian Academy of Sciences, Oktyabrya Ave. 71, 450054 Ufa, Russia

⁵ Institute for Applied Materials - Applied Materials Physics, Karlsruhe Institute of Technology, Hermann-von-Helmholtz-Platz 1, 76344 Eggenstein-Leopoldshafen, Germany

⁶ Ufa State Aviation Technical University, Karl Marx St. 12, 450008 Ufa, Russia

Received 19 April 2022 / Accepted 15 June 2022 / Published online 5 July 2022

© The Author(s), under exclusive licence to EDP Sciences, SIF and Springer-Verlag GmbH Germany, part of Springer Nature 2022

Abstract. A general approach is applied to study a new type of intrinsic spatially localized vibrational modes in a defect free nonlinear crystal lattice, i.e., discrete breathers (DBs). For that, dynamics of eight delocalized nonlinear vibrational modes (DNVMs) of two-dimensional triangular lattice is investigated in three-dimensional single crystal of hcp Ti. Molecular dynamics simulations are performed using two interatomic potentials (Ti_EAM and Ti_MEAM). The eight DNVMs modeled with Ti_EAM potential are found to be unstable and dissipate their vibrational energy very rapidly. The usage of Ti_MEAM interatomic potential allows to excite stable two-dimensional (planar) DBs. These localized vibrational modes can be called DBs, since the frequency of atomic oscillations is above the upper edge of the phonon spectrum of Ti, and the atomic oscillations are localized in one spatial direction and delocalized in the other two directions. The lifetimes of the two-dimensional DBs are in the range of 5–14 ps, while the maximal lifetime of DBs excited on the basis of DNVM 7 is circa 28 ps. These DBs can accumulate vibrational energy, which is in the range of 0.1–0.5 eV per atom. The stable two-dimensional DBs are characterized by a hard type of nonlinearity. A comparison with analogous two-dimensional DBs in fcc metals are undertaken. The obtained results make a significant contribution to the study of DBs in metals and will be important for understanding the influence of intrinsic localized vibrational modes on the physical properties of materials.

1 Introduction

Considerable attention in solid-state physics is paid to the study of crystal lattice oscillations. Under extreme conditions, such as irradiation with high-energy particles, elevated temperatures, severe plastic deformation etc., the anharmonism of interatomic interactions should be taken into account. Many fundamental characteristics of crystals (heat capacity, thermal expansion, changes of the elastic constants) can be determined due to analysis of atomic oscillations.

About three decades ago, it was shown that, in addition to phonon wave packets, nonlinear defect-free lattices are capable of supporting a fundamentally new type of vibrational modes, which were called intrinsic localized modes or discrete breathers (DBs), whose contribution to crystal physics has yet to be described.

On the other hand, Chechin et al. developed a general method for finding exact solutions to nonlinear equations of atomic motion in the form of delocalized nonlinear vibrational modes (DNVMs) for lattices of any dimension [1–3]. This method is based on group theory applied to the analysis of lattice point symmetry. DNVMs are completely determined by the lattice symmetry and exist as exact solutions for any type of interatomic potential and any amplitude [1–3]. The simplest example of DNVM in a nonlinear chain of particles is the zone-boundary mode, where the displacement of the n th particle from its equilibrium lattice site is described as $u_n(t) = (-1)^n A \sin \omega t$. If this mode has a frequency above the phonon spectrum of the chain, which is the case for hard-type anharmonic interactions, an approximate DB solution can be obtained by introducing the following localizing function with radial symmetry: $u_n(t) = (-1)^n A \sin \omega t / \cosh(\beta n)$. This approach (application of the localizing function on the DNVMs with the frequencies above the upper edge of the phonon spectrum) was used to find a number of DBs

^a e-mail: obachurina@yahoo.com (corresponding author)

in the triangular β -FPU (Fermi-Pasta-Ulam) lattice [4] and in bcc vanadium and niobium [5].

Spontaneous thermofluctuational generation is the most natural way to excite DBs in crystals [6–8]. An increase of the temperature results in an increase of the probability of the thermofluctuational excitation of a DB [8, 9], but at the same time it reduces the DB lifetime due to energy dissipation via interaction with neighboring atoms oscillating with larger amplitudes.

An n -dimensional lattice can support k -dimensional DBs ($k < n$), which are delocalized in k dimensions and localized in $(n - k)$ dimensions. The most studied currently are zero-dimensional DBs spatially localized in all n dimensions [10–19]. One-dimensional DBs in two-dimensional triangular lattice are localized only in one dimension [20], so that in this case $n = 2$ and $k = 1$. The case of $n = 3$ and $k = 1$, i.e., one-dimensional DB, in three-dimensional fcc metals was considered in Ref. [4]. Planar DBs ($k = 2$) in three-dimensional ($d = 3$) fcc metals were investigated in Ref. [21]. As it was recently found out, DBs can exist near crystal surface in Pt₃Al intermetallic alloy [22]. It is quite probable that the DBs in free-standing graphene reported by Fraile et al. [10] can be obtained by imposing a localizing function on one of the DNVMs of hexagonal lattice, although this hypothesis needs to be verified.

DBs have been found experimentally in atomic wave packets [23], arrays of superconducting Josephson junctions [24–26], periodic nonlinear electric chains [27], etc. In a recent theoretical work [28], the possibility of existence of DBs in a chiral helimagnet was discussed.

Another mechanism of DB generation is associated with its spontaneous appearance due to the modulational instability of the DNVM [29–31], which leads to a spatial localization of the vibrational energy, i.e., formation of DBs. They slowly emit their energy in the form of small amplitude waves thus contributing to a transition of the system to thermal equilibrium. The modulational instability of various DNVMs was studied in a two-dimensional hexagonal lattice described by a pair potential with a quartic hard-type nonlinearity [32]. The authors found that if the atoms vibrate with a frequency outside the phonon spectrum of the crystal, and their amplitudes are smaller than a certain threshold value, the vibrational energy is not transferred into the rest of the crystal in the form of small-amplitude oscillations. Due to the fact these DNVMs can exist for a relatively long period time without interacting with other “unperturbed” atoms.

Recently, it was established that two-dimensional DBs can be excited in a (111) close-packed atomic plane based on four out of eight one-component DNVMs in defect-free fcc metals (Al, Cu, Ni). Thus excited DBs are characterized by a hard type of nonlinearity, can accumulate vibrational energy of the order of 0.6–1.5 eV per atom and have the lifetimes in the range of 24–47 ps [33]. As a continuation of the above cited work, Bachurina and Kudreyko demonstrated that two-dimensional DBs can be also excited based on one selected two-component DNVM in the same fcc metals [34]. Note, that one-component DNVM is named this way due to

the fact that it is characterized by a single parameter, which is the amplitude of atomic oscillations from the equilibrium lattice sites. By analogy, two-component DNVM is described by two parameters, which determine two different atomic oscillation amplitudes within the same DNVM. In this case, the first group of atoms is characterized by one value of the displacement amplitude, while the second group—by another value. As was demonstrated in the recent publication [4], the same crystal lattice can support various types of DBs, and therefore, elucidation of their effect on materials properties is an actual task.

For a time being, the systematic study of two-dimensional DBs excited based on one- and two-component DNVMs was performed only for fcc metals, while similar investigations for metals with a different crystal lattice are absent. It will not be superfluous to say that the type of crystal lattice and the corresponding symmetry largely determine the properties and characteristics of DBs. Therefore, the main goal of the present work is to study two-dimensional DBs excited based on eight one-component DNVMs in a three-dimensional hcp single crystals of Ti with the help of molecular dynamics simulations. To elucidate how the choice of interatomic potential can influence the possibility of existence of two-dimensional DBs, all calculations are carried out for two different Ti potentials.

2 Delocalized nonlinear vibrational modes and simulation details

Eight one-component DNVMs in a two-dimensional triangular lattice derived by Chechin and Ryabov [3] are presented in Fig. 1. The x -axis is directed along the horizontal atomic rows, the y -axis is perpendicular to the x -axis and is along the vertical atomic rows, and the z -axis is perpendicular to the plane of the figure. The basal plane (0001) in hcp crystal is equivalent to two-dimensional triangular lattice, and therefore, the DNVMs can be used as starting points to excite two-dimensional DBs in hcp lattice. It is worth noting that the same DNVMs can be used for excitation of DBs in fcc lattice, inasmuch as basal plane (0001) in hcp lattice is equivalent to a close-packed (111) plane in fcc crystal. At that, the atomic packing above and below this chosen plane in hcp and fcc lattices are certainly different.

According to the results obtained in Ref. [4], DNVMs 1, 2, 4, 5 are symmetrical, while DNVM 3, 6, 7, 8 are asymmetrical ones. The main difference is that the symmetric modes have equal in absolute value maximal positive and negative displacements from the equilibrium lattice sites, and asymmetrical ones, on the contrary, have unequal positive and negative displacements. As was already pointed out in our previous publication [33], initiation of atomic displacements along “the short” arm of asymmetrical DNVMs results in an intensive energy

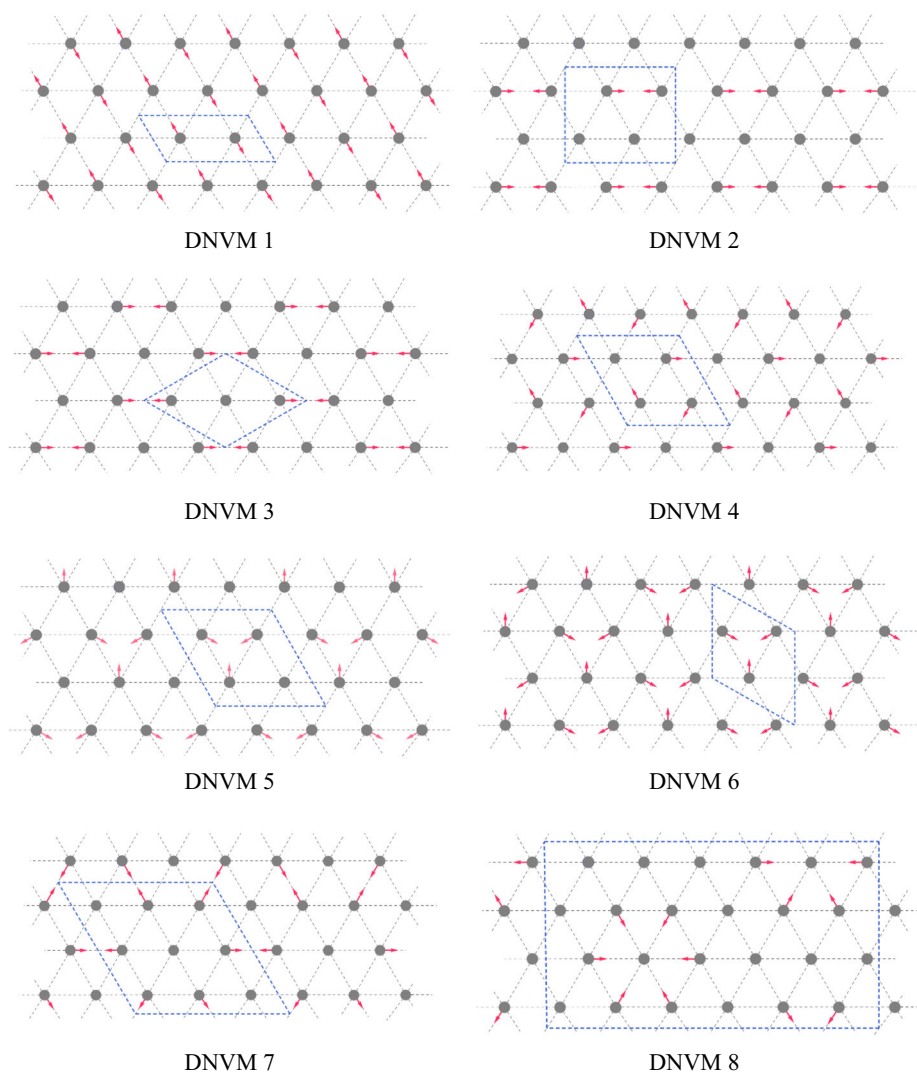
dissipation and, as a consequence, an instability of these DNVMs. Based on this, atomic displacements in all four asymmetrical DNVMs 3, 6, 7, 8 are initiated along “the long” arm. Thus, these eight DNVMs are excited in the same basal plane, and then their lifetimes, frequency, energy and oscillation amplitude are analyzed.

Large-scale Atomic/Molecular Massively Parallel Simulator (LAMMPS) [35] is applied for molecular dynamics simulations. Two different interatomic potentials for hcp Ti are taken from the LAMMPS library. The first one is a many-body parametrized semi-empirical potential of the Finnis–Sinclair type based on the embedded atom method (EAM) (designated throughout the paper for brevity as Ti_EAM) [36], and the second one combines the modified embedded-atom method (MEAM) and the Stillinger–Weber potentials (designated as Ti_MEAM) [37]. The MEAM potential is a modification of the EAM potential and includes directional bonds, the change in the angle between them contributes to the interaction energy. The equilibrium lattice constants at zero temperature reproduced by the

Ti_EAM interatomic potential are $a = 2.967 \text{ \AA}$ and $c/a = 1.592$, and by the Ti_MEAM potential are $a = 2.931 \text{ \AA}$ and $c/a = 1.596$.

To find initial conditions at which stable DBs can exist, variation of the amplitudes of atomic displacements in the relatively wide range of $0.05\text{--}0.5 \text{ \AA}$ are carried out. Only atoms belonging to the corresponding DNVMs (marked with arrows in Fig. 1) are displaced, while the other atoms have zero initial displacements. At the initial moment of time, all atoms in the computational cell have zero velocities. The time step is 1 fs, which is small enough for this type of simulations. Periodic boundary conditions are applied along all the three coordinate directions. Molecular dynamics simulations are performed at initial temperature $T = 0 \text{ K}$, and the NVE thermodynamic ensemble (constant number of atoms, volume, and energy) is applied. Zero temperature is used to avoid the thermal fluctuations which significantly disturb oscillation of DNVM atoms and thus can decrease their lifetime drastically.

Fig. 1 Eight one-component DNVMs in two-dimensional triangular lattice derived in Ref. [3]. The DNVMs 1, 2, 4, 5 are symmetrical, while the DNVM 3, 6, 7, 8 are asymmetrical. The red arrows show atomic displacements from the equilibrium lattice sites. The blue dashed lines indicate the unit cells of the vibrational state in the considered plane. At the initial moment of time, the length of all displacement vectors for each mode is the same and equal to A . The presented schemes demonstrate only the part of a basal plane inside the three-dimensional computational cell



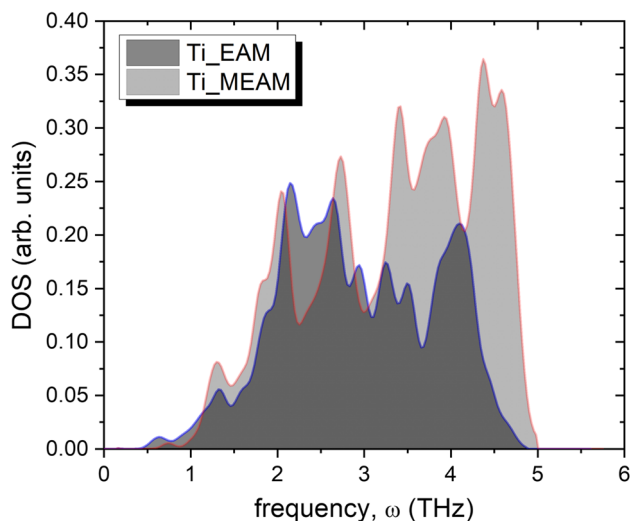


Fig. 2 Phonon density of states (DOS) of hcp Ti calculated with the use of the two interatomic potentials Ti_EAM and Ti_MEAM. The upper edges of the phonon spectrum reproduced by the potentials are 4.9 THz (Ti_EAM) and 5.0 THz (Ti_MEAM)

All simulations are limited to 4×10^4 time steps (corresponding to 40 ps of simulation time), which is enough for observation of the studied phenomena.

Calculation of the phonon density of states (DOS) are carried out by means of the standard method implemented in LAMMPS. The Green's function molecular dynamics method is applied to compute the dynamical matrix based on fluctuation–dissipation theory for a group of atoms (for detail see Refs. [35, 38]). The Green's function is measured every 10 time steps. Totally 10 million time steps at a constant temperature of 20 K using NVT thermodynamic ensemble (constant number of atoms, volume, and temperature) are performed. The results of DOS calculation for both interatomic potentials are demonstrated in Fig. 2. Thus the upper edges of the phonon spectrum are found to be 4.9 THz for the Ti_EAM potential and 5.0 THz for the Ti_MEAM potential.

The sizes of the computational cells corresponding to various DNVs, the number of atoms in them, equilibrium lattice constants at $T = 0$ K, and the upper edge of phonon spectrum for Ti_EAM and Ti_MEAM potentials are summarized in Table 1. Note that computational cells for asymmetrical DNVs 3, 6, 7, 8 are different from those used for symmetrical DNVs 1, 2, 4, 5. This is obviously due to the different periods of the unit cells of the vibrational state for symmetrical and asymmetrical DNVs.

3 Simulation results and discussion

In the following paragraphs the results obtained for both used interatomic potentials Ti_EAM and Ti_MEAM are presented and discussed separately.

3.1 Ti_EAM potential

Molecular dynamics simulations demonstrate that no excitation of stable two-dimensional DBs in hcp Ti on the basis of both symmetrical and asymmetrical DNVs occurs. To illustrate this fact, Fig. 3a displays the time dependence of the kinetic energy of the ten consecutive atoms along the direction perpendicular to the close-packed plane, where DNV 2 were excited at the initial amplitude of $A = 0.25$ Å. At that, atom numbered as 1 is located in the base plane, i.e., it belongs to the DNV. It should be noted that energy dissipation takes place symmetrically with respect to the base plane, and therefore, only the results for the atoms located above this plane are presented. As clearly shown in Fig. 3a, right after the onset of the simulation, the kinetic energy of atom 1 reduces almost linearly in time, which is associated with the dissipation of the vibrational energy and its transfer onto the neighboring atomic planes. This is confirmed by that fact that vibrational energy of atom 2 noticeably increases and is about of 10% of the initial energy of atom 1 and experiences characteristic irregular jumps. The vibrational energy of atom 3 increases, reaches a maximum, and then decreases, as shown in Fig. 3a. Moreover, the maximum of the vibrational energy of atom 3 exactly corresponds to the time instant, when atom 1 transferred to the crystal all its kinetic energy, which became almost equal to zero. An increase in the energy of atom 3 is accompanied by the subsequent transfer of the vibrational energy to the neighboring atomic planes, where atoms 4–10 are located. As also clearly presented in Fig. 3a, atoms 4–10 are at rest until an excitation wave, which is due to the destruction of the DNV 2, comes to them and increases their oscillation amplitudes significantly. Thus the energy dissipation occurs in the direction perpendicular to the DNV plane. Since the size of the computation cell is finite along the y -axis, and periodic boundary conditions are used, two excitation waves reach the upper and the lower edges of the cell, enter the cell again from opposite sides and then continue their motion through the crystal. This is the reason for the appearance of the second and the third bursts of vibrational energy for atoms 1, 3, 5, 6, and 8, for which they are especially clearly visible. Similar results were obtained for the other both symmetrical and asymmetrical DNVs presented in Fig. 1, with the difference that DBs decay occurred in a shorter time of approximately 1 ps, i.e., about 10 atomic oscillations.

Since, as it turned out, attempts to excite the stable two-dimensional DBs using Ti_EAM potential were not successful, the possibility of such an excitation using Ti_MEAM potential are studied in detail in the following paragraph. It is worth noting that a similar phenomenon, when in the same material DBs can be excited with one potential and cannot be excited with another one, has already been noted earlier. For example, DBs in diamond could not be excited using Tersoff interatomic potential [39], while Hizhnyakov et al. [40, 41] managed to excite DBs employing the more advanced long-range carbon bond-order potential

Table 1 Lattice constants a_0 (in Å) and c_0/a_0 at $T = 0$ K, the upper edge of phonon spectrum ω (in THz), the sizes of the three-dimensional computational cells along the x -, y - and z -directions (in Å) and the number of atoms (N) in the cells used for calculation of eight DNVMs in hcp Ti for the two different interatomic potentials

Metal	a_0	c_0/a_0	ω	Computational cell ($x \times y \times z$)		N	
				DNVMs 1, 2, 4, 5	DNVMs 3, 6, 7, 8	DNVMs 1, 2, 4, 5	DNVMs 3, 6, 7, 8
Ti_EAM	2.967	1.592	4.9	$29.3 \times 50.8 \times 49.8$	$35.2 \times 50.8 \times 49.8$	4000	4800
Ti_MEAM	2.931	1.596	5.0	$29.3 \times 50.8 \times 49.8$	$35.2 \times 50.8 \times 49.8$	4000	4800

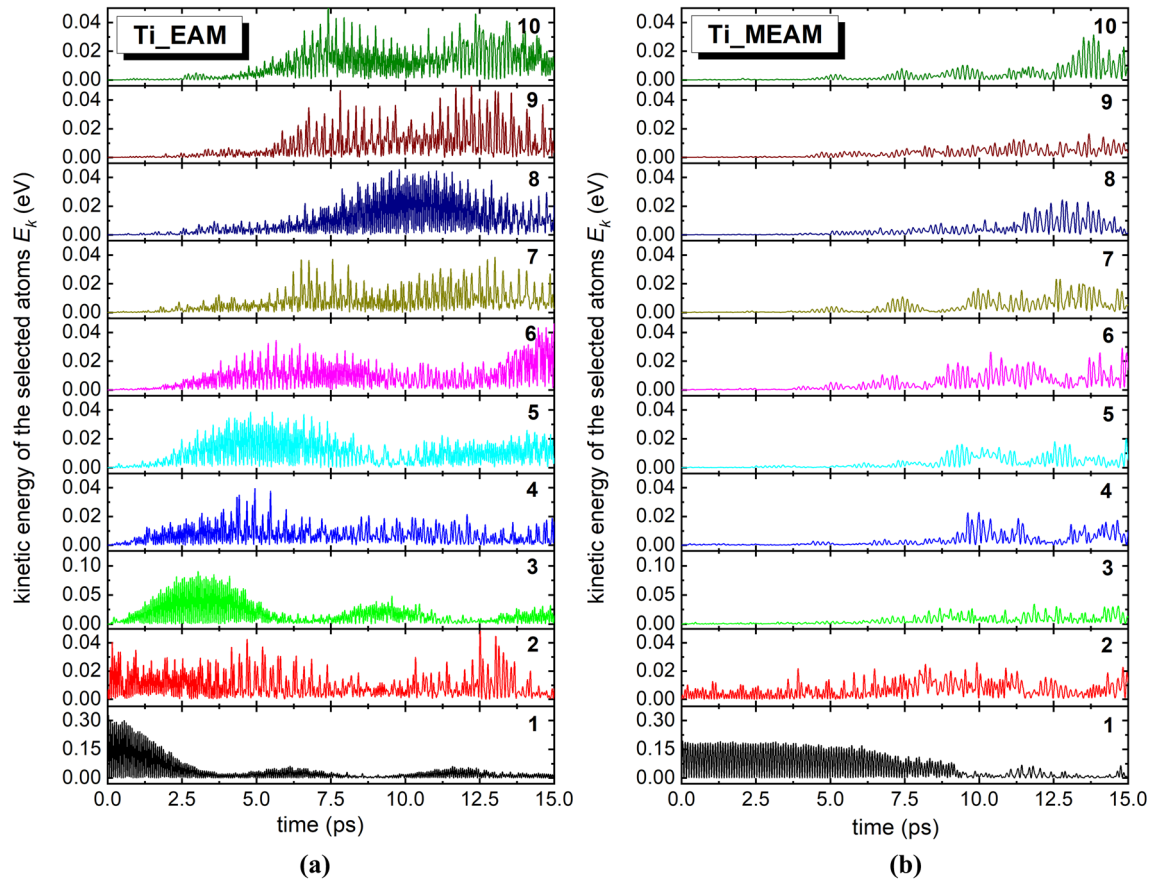


Fig. 3 Time dependence of the kinetic energy of the ten selected atoms along the direction perpendicular to the DNV plane calculated using the two interatomic potentials **a** Ti_EAM and **b** Ti_MEAM. The initial amplitude $A = 0.25$ Å is used for both interatomic potentials. Atom numbered as 1 belongs to the close-packed atomic plane, where symmetrical DNV 2 is excited, while atoms 2–10 are above this plane

(LCBOP) [42]. The latter in contrast to the “simple” Tersoff potential, describes the orientation of bonds and switching-off effects in a more accurate way.

3.2 Ti_MEAM potential

Each considered DNV has its own amplitude range in which it can be excited. Large-amplitude atomic oscillations are localized along one spatial z direction and delocalized along the two other x and y directions in three-dimensional single crystal. The studied DNVs

remain in the atomic plane, where they were initially excited. The amplitudes of atomic oscillations exponentially decrease with distance from this plane, and therefore, these DNVs can be called two-dimensional DBs. The latter is stable (or long-lived) two-dimensional (or in-plane excited) DB in the case when the following three conditions are satisfied: (1) the lifetime exceeds 5 ps (circa 40 oscillations); (2) the frequency of atomic

Table 2 Summary of the simulation results for eight DNVMs in hcp Ti calculated with the use of Ti_MEAM interatomic potential. The symmetry of DNVMs and stability of excited on their basis two-dimensional DBs are given. The range of initial amplitudes (in Å) at which stable (or long-lived) two-dimensional DB can be excited, and maximal lifetime for the used computational cell are also presented

DNVM	Symmetry	Stability	Amplitude range (Å)	Maximal lifetime (ps)
1	Symmetrical	No	–	–
2	Symmetrical	Yes	$0.2 \leq A \leq 0.4$	8.9
3	Symmetrical	No	–	–
4	Asymmetrical	No	–	–
5	Symmetrical	Yes	$0.15 \leq A \leq 0.4$	13.8
6	Asymmetrical	Yes	$0.1 \leq A \leq 0.35$	11.3
7	Asymmetrical	Yes	$0.1 \leq A \leq 0.5$	27.9
8	Asymmetrical	No	–	–

oscillations is above the upper edge of the phonon spectrum of the crystal; (3) the frequency of atomic oscillations increases with increasing amplitude, i.e., corresponds to a hard type of nonlinearity, which is found to be typical for pure metals with different crystal lattices and is related to the screening of the ion-ion interaction by the conduction electrons [43, 44].

Stable two-dimensional DBs can be excited only on the basis of DNVMs 2 and 5–7, while DNVMs 1, 3, 4 and 8 fades out and dissipate their vibrational energy almost immediately after a few oscillation periods. The simulation results obtained for the eight DNVMs excited employing Ti_MEAM interatomic potential are summarized in Table 2.

Figure 4 demonstrates the dependences of the lifetime, oscillation frequency, kinetic energy per oscillating atom, and steady-state amplitude for the stable DNVMs 2, 5–7 vs. initial amplitude A . The lifetimes of the studied DNVMs are in the range of 5 to 14 ps. The only exception is DNVM 7 excited with the initial amplitude of $A = 0.2$ Å, which has the lifetime of 28 ps (see Fig. 4a). It should be noted that in the range of initial amplitudes of 0.25–0.5 Å, DNVM 3 has the lifetime less than 5 ps, i.e., it is just at the lower limit of the lifetime defined above, and therefore, it cannot be considered as a stable DB. Despite the fact that the lifetime is used as a parameter for characterizing DB stability, it should be borne in mind that this parameter is a conditional factor, since an increase of the size of the computational cell results in an increase of the DB lifetime. This, for example, was recently discovered for a linear (rod-like) DB in fcc Ni [20]. Nevertheless, it should be pointed out that long-lived DBs excited in the computational cell of one size remain long-lived ones in the cells of the larger size. Hence, DB lifetime can be considered as a qualitative parameter when characterizing nonlinear vibrational modes.

DB decay occurs at a certain moment of time by the deviation of one (or several) oscillating atoms from a given displacement vector. The latter is associated with the loss of vibrational energy due to interaction with

neighboring atoms and causes a cascade of displacements, which propagates very quickly in a given plane containing excited atoms.

The dependence of the oscillation frequency of DNVMs, ω , vs. initial amplitude A is presented in Fig. 4b. Note that excitation of any type of DBs occurs when its frequency is above the upper edge of the phonon spectrum of low-amplitude oscillations of the crystal lattice, which is about 5 THz (see Fig. 2). Moreover, the deviation of the DB frequency from the spectrum is due to its dependence on the amplitude. If the DB frequency increases (decreases) with the amplitude, then DB exhibits a hard (soft) type of nonlinearity. As clearly shown in Fig. 4b, all DNVMs demonstrate a hard type of nonlinearity. In contrast to fcc metals [20, 21, 33], hcp Ti does not exhibit a sharp increase in the frequency of vibrational modes. For instance, in the range of the investigated amplitudes, the frequency of two-dimensional DB in Ti increases from 6 to 8.5 THz, while from 9 to 18 THz in fcc Ni [33].

Figure 4c shows the dependence of the kinetic energy of two-dimensional DBs on the initial amplitude. The energy increases with the increase in amplitude. In the range of low initial amplitudes ($A \leq 0.2$ Å), the data points for different DNVMs are overlay each other, suggesting that in this amplitude range all considered DNVMs have similar ability to accumulate vibrational energy. However, at higher initial amplitudes ($A > 0.2$ Å), vibrational energy per atom in the different DNVMs differs significantly. For example, at maximal investigated amplitude of $A = 0.5$ Å, the highest vibrational energy per atom in DNVM 2 is of about 0.5 eV, which is approximately two times higher than that for DNVMs 6 and 7.

The steady-state amplitude of the stable DBs excited on the basis of one-component DNVMs as a function of the initial amplitude is demonstrated in Fig. 4d. This steady-state oscillation amplitude is determined by averaging the span of DNVM atomic oscillations at a time of 1 ps after the onset of simulation. As seen, for all presented DBs, initial amplitude is always less than steady-state amplitude, which is set after several

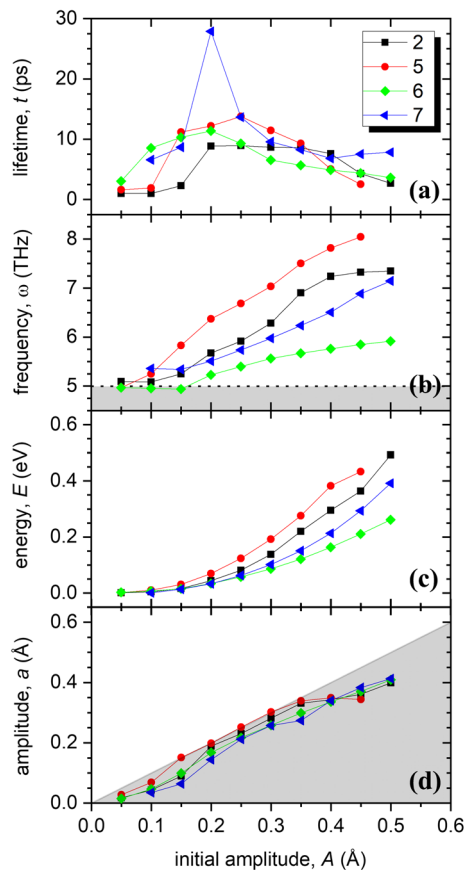


Fig. 4 Lifetime (a), oscillation frequency (b), kinetic energy per oscillating atom (c), and steady-state amplitude vs. initial oscillation amplitude A calculated in hcp Ti using the Ti_MEAM interatomic potential. The numbers in the legend correspond to the number of one-component DNVMs illustrated in Fig. 1, which are used for excitation of two-dimensional DBs. The results are presented only for stable two-dimensional DBs. The gray area in **b** shows the frequency region below the upper edge of the phonon spectrum of hcp Ti. The gray area in **d** indicates the region, where $a \leq A$, demonstrating the fact that DBs always dissipate their initial vibrational energy. The solid lines interpolating the data points are guides to the eye

oscillations. It is due to the fact that DBs dissipate their vibrational energy onto neighboring atoms. This ability of different two-dimensional DBs to dissipate energy is very different. In the range of initial amplitudes from 0.2 to 0.35 Å, DBs excited on the basis of DNVMs 2, 5–7 weakly dissipate their vibrational energy, and therefore, the points are located very close to the line $a = A$ (see Fig. 4d). It should be mentioned that wrong choice of the arm of initial displacements for asymmetric DNVMs can result in outwardly paradoxical fact, when the steady-state amplitude is higher than the initial one, i.e., $a > A$. It is for this reason that the initial displacements of the atoms in the asymmetric modes are set along the “long” arm in the present study.

Figure 3b presents the time dependence of the kinetic energy of the ten consecutive atoms along the direction

perpendicular the plane, where DB was excited based on DNVm 2 with the initial amplitude of $A = 0.25$ Å, but for Ti_MEAM interatomic potential. In contrast to Ti_EAM (Fig. 3a), oscillations of the kinetic energy continue up to 8.9 ps, which is the lifetime of this two-dimensional DB. Oscillation amplitudes of the atoms 2–10 are at least one order of magnitude lower than that for atom 1 belonging to DNVm 2 and begin to increase only after 7 ps. The latter is an indicator that the DB begins to disintegrate and dissipate its vibrational energy over the volume of the single crystal. First the energy is transferred onto the nearest atomic planes and then spreads to the next ones. Note again that the amplitudes of atomic oscillations in the adjacent rows rapidly decrease with increasing distance from the plane, where the DB was initially excited. For instance, the oscillation amplitude is circa 0.2 Å in the base plane and it is 0.02 Å in the second one. In the third and subsequent atomic planes the oscillation amplitudes are already indistinguishable from zero (see Fig. 3b). Thus, atomic oscillations drastically decrease with the distance from the base atomic plane, i.e., they are strongly localized, and therefore, these DNVMs can be considered as two-dimensional (planar) DBs.

Two symmetrical DNVMs (1 and 3) and two asymmetrical DNVMs (4 and 8) turn out to be unstable, while the other two symmetrical and two asymmetrical DNVMs are stable. The longest lifetime has DB excited based on asymmetric DNVm 7, which looks like a burst in Fig. 4a. From the results presented in Fig. 4, it is impossible to make an unambiguous conclusion that DBs excited with asymmetrical DNVMs have a longer lifetime. In contrast to asymmetrical modes, symmetrical DNVMs, as a rule, have higher oscillation frequencies and are more distant from the upper edge of the phonon spectrum (Fig. 4b). At high initial amplitudes, the highest vibrational energy per atom can be accumulated by the symmetrical DNVm 2, and the lowest by asymmetrical DNVm 7. The energy values of the other DNVMs are between them. Here, it is also impossible to draw any conclusion about the influence of mode symmetry on the ability to accumulate vibrational energy. Thus, it can be concluded that long-lived DB in hcp Ti is one whose atomic oscillation frequency is slightly above the upper edge of the phonon spectrum, and one that accumulates vibrational energy poorly. It follows from the foregoing that, based on the symmetry of the vibrational modes, it is impossible to say in advance which of them will give the most long-lived DBs. Therefore, it is necessary to investigate in each material all possible DNVMs allowed by the symmetry of a given crystal.

Since at present there are no results of studying two-dimensional DBs in other hcp metals, let us compare the obtained results with those of the work [33], where the possibility of excitation of two-dimensional DBs based on the same eight one-component DNVMs in fcc metals (Al, Cu, Ni) was explored. It should be recalled that the two-dimensional triangular lattice for which these eight DNVMs were calculated in Ref. [33] is equivalent to a close-packed (111) plane in fcc crystal

and (0001) plane in hcp crystal. For simplicity of visual comparison, the present work uses the same numbering of DNVMs as the cited above. In all studied fcc metals, DBs excited on the basis of DNVMs 1, 4, 6, 8 turned out to be unstable and rapidly decayed. That is, three DNVMs (1, 4, 8) are unsuitable for excitation of DBs in both Ti and the mentioned fcc metals. The lifetime of DBs for the fcc metals is characterized by a pronounced peak in the range of initial amplitudes from 0.15 to 0.25 Å. The same is valid for hcp Ti (see Fig. 4a). The most long-lived DBs in fcc metals are those excited on the basis of DNVMs 2 and 5. They are characterized by a higher frequency and dissipate less energy, in contrast to the other DNVMs. In Ti, these DNVMs give rise to DBs with an average lifetime. DNVN 7 in fcc metals is stable, but it can accumulate larger energy, and the oscillation frequency is not much higher than the upper edge of the phonon spectrum. In addition, DNVN 2 in fcc metals is characterized by the least scattering of vibrational energy (see Fig. 4 in Ref. [33]). In Ti this is true for DNVN 5, while DNVN 2 dissipates more energy. Thus, as can be seen from the comparison performed above, the general trends between two-dimensional DBs in hcp and fcc metals, although traced, are not completely observed. This is, of course, primarily due to the peculiarities of the crystal lattice of the studied metals.

The fact that the excitation of stable DBs based on the eight DNVNs does not occur when using the Ti_EAM interatomic potential, in contrast to the Ti_MEAM potential, can be explained mainly as follows. Since the Ti_MEAM potential takes into account directional bonds and changes in the angle between them, this means that with a slight deviation of the oscillating atom from the initial plane of the mode, this will lead to a change in the directional angles between the bonds and, accordingly, to an increase in the attraction forces of atoms located in the same atomic plane, that is, to increasing of interaction energy. Thus, the contribution to the increase in energy occurs due to a change in the density of the electron cloud and a change in the directional bond angles. The latter means that this atom will tend to reduce its potential energy and, therefore, return to the original atomic plane. In the absence of a contribution from the directional bonds, i.e., as in the case of the Ti_EAM potential, only a change in the density of the electron cloud makes a contribution to the energy increase. From which it can be concluded that, due to its peculiarity, the Ti_MEAM potential is more suitable for modeling intrinsic localized modes in hcp Ti, in contrast to the Ti_EAM potential. The question of how these two interatomic potentials will manifest themselves in the simulation of DBs of various types in other metals with hcp crystal lattice remains open at present and requires further research.

4 Conclusions

In the present work, a general approach was applied to find new type of DBs via investigation of stability of eight one-component DNVNs in three-dimensional single crystal of hcp Ti. Molecular dynamics simulations were performed with the use of two interatomic potentials (Ti_EAM and Ti_MEAM). The main findings can be formulated as follows. Both symmetrical and asymmetrical DNVNs modeled with Ti_EAM potential are unstable. They dissipate their initial vibrational energy and decay within the first 10 atomic oscillations. Stable two-dimensional (planar) DBs in hcp Ti were successfully excited based on four out of the eight considered DNVNs (2, 5–7) using Ti_MEAM interatomic potential. Atomic oscillations of these DBs exponentially decrease with the distance from the excited atomic plane and are localized in one direction and delocalized in the other two spatial directions. DNVNs 1, 3, 4, 8 are found to be unstable and rapidly dissipate their vibrational energy. The lifetimes of the studied two-dimensional DBs are in the range of 5–14 ps, with the only exception, the lifetime of DNVN 7 is of about 28 ps. Vibrational energy that can be accumulated by oscillating atoms is of the order of 0.1–0.5 eV per atom. The frequency of atomic oscillation is above the upper edge of the phonon spectrum of Ti, which is at about 5 THz. DBs excited based on DNVNs 2, 5–7 weakly dissipate their vibrational energy. All observed stable two-dimensional DBs are of a hard type of nonlinearity, i.e., the frequency of atomic oscillations increases with the oscillation amplitude. At the present stage of research, it is impossible to draw an unambiguous conclusion about the influence of DNVN symmetry on the stability of a two-dimensional DB excited on its basis. The impossibility of exciting a DB using the Ti_EAM potential is explained primarily by its peculiarity and difference from the Ti_MEAM potential.

The results obtained on the possibility of exciting new types of DBs in hcp Ti make a significant contribution to the foundation of the theory of DBs in metals. For that it is necessary to have more extensive data on nonlinear vibrational modes of various dimensions in materials with different crystal lattices. However, this requires additional research, in particular, for hcp metals, for which there are currently no such studies. In addition, it seems interesting to expand our understanding of the possibility of exciting DBs in hcp Ti based on two-component modes, which is an interesting topic for a separate study. The works in this direction will help to answer the question on how DBs affect macroscopic properties of crystals [45, 46].

Acknowledgements OVB and SVD work was supported by the Russian Science Foundation, Grant no. 21-12-00229. RTM's work was accomplished in terms of the State Assignment of the Institute for Metals Superplasticity Problems of the Russian Academy of Sciences financed by the Ministry of Science and Higher Education of the Russian Federation (Registration No. AAAA-A17-117041310220-8). DVB

acknowledges the support within the framework of work on the state task of the Ministry of Science and Higher Education of the Russian Federation for FGBOU VO "UGATU" (agreement No. 075-03-2021-014/4) in youth research laboratory "Metals and Alloys under Extreme Impacts".

Author contributions

All the authors were involved in the preparation of the manuscript. All the authors have read and approved the final manuscript.

Data availability statement The raw/processed data required to reproduce these findings cannot be shared at this time as the data also forms part of an ongoing study.

References

1. V.P. Sakhnenko, G.M. Chechin, Bushes of modes and normal modes for nonlinear dynamical systems with discrete symmetry. *Phys. Dokl.* **39**, 625 (1994)
2. G.M. Chechin, V.P. Sakhnenko, Interactions between normal modes in nonlinear dynamical systems with discrete symmetry. Exact results. *Physica D* **117**(1–4), 43–76 (1998)
3. G.M. Chechin, D.S. Ryabov, S.A. Shcherbinin, Nonlinear vibrational modes in graphene: group-theoretical results. *Lett. Mater.* **6**, 9–15 (2016)
4. R.I. Babicheva, A.S. Semenov, E.G. Soboleva, A.A. Kudreyko, K. Zhou, S.V. Dmitriev, Discrete breathers in a triangular b-Fermi–Pasta–Ulam–Tsingou lattice. *Phys. Rev. E* **103**, 052202 (2021)
5. K.A. Krylova, I.P. Lobzenko, A.S. Semenov, A.A. Kudreyko, S.V. Dmitriev, Spherically localized discrete breathers in bcc metals V and Nb. *Comput. Mater. Sci.* **180**, 109695 (2020)
6. M.E. Manley, A.J. Sievers, J.W. Lynn, S.A. Kiselev, N.I. Agladze, Y. Chen, A. Llobet, A. Alatas, Intrinsic localized modes observed in the high-temperature vibrational spectrum of NaI. *Phys. Rev. B* **79**(13), 134304 (2009)
7. M. Eleftheriou, S. Flach, Discrete breathers in thermal equilibrium: distributions and energy gaps. *Physica D-Nonlinear Phenomena* **202**(1–2), 142–154 (2005)
8. L.Z. Khadeeva, S.V. Dmitriev, Lifetime of gap discrete breathers in diatomic crystals at thermal equilibrium. *Phys. Rev. B* **84**(14), 144304 (2011)
9. M. Eleftheriou, S. Flach, Interaction of discrete breathers with thermal fluctuations. *Low Temp. Phys.* **34**(7), 554–558 (2008)
10. A. Fraile, E.N. Koukaras, K. Papagelis, N. Lazarides, G.P. Tsironis, Long-lived discrete breathers in free-standing graphene. *Chaos Solitons Fractals* **87**, 262–267 (2016)
11. O.V. Bachurina, R.T. Murzaev, A.S. Semenov, E.A. Korznikova, S.V. Dmitriev, Properties of moving discrete breathers in beryllium. *Phys. Solid State* **60**(5), 989–994 (2018)
12. S.V. Dmitriev, L.Z. Khadeeva, A.I. Pshenichnyuk, N.N. Medvedev, Gap discrete breathers in two-component three-dimensional and two-dimensional crystals with Morse interatomic potentials. *Phys. Solid State* **52**(7), 1499–1505 (2010)
13. A. Riviere, S. Lepri, D. Colognesi, F. Piazza, Wavelet imaging of transient energy localization in nonlinear systems at thermal equilibrium: the case study of NaI crystals at high temperature. *Phys. Rev. B* **99**, 024307 (2019)
14. S.V. Dmitriev, E.A. Korznikova, Y.A. Baimova, M.G. Velarde, Discrete breathers in crystals. *Phys. Uspekhi* **59**, 446–461 (2016)
15. A.A. Kistanov, Y.A. Baimova, S.V. Dmitriev, A molecular dynamics study of [111]-polarized gap discrete breathers in a crystal with NaCl-type structure. *Tech. Phys. Lett.* **38**(7), 676–679 (2012)
16. A.A. Kistanov, R.T. Murzaev, S.V. Dmitriev, V.I. Dubinko, V.V. Khizhnyakov, Moving discrete breathers in a monoatomic two-dimensional crystal. *JETP Lett.* **99**(6), 353–357 (2014)
17. R.T. Murzaev, R.I. Babicheva, K. Zhou, E.A. Korznikova, S.Y. Fomin, V.I. Dubinko, S.V. Dmitriev, Discrete breathers in alpha-uranium. *Eur. Phys. J. B* **89**(7), 1–6 (2016)
18. R.T. Murzaev, D.V. Bachurin, E.A. Korznikova, S.V. Dmitriev, Localized vibrational modes in diamond. *Phys. Lett. A* **381**(11), 1003–1008 (2017)
19. R.T. Murzaev, A.A. Kistanov, V.I. Dubinko, D.A. Terentyev, S.V. Dmitriev, Moving discrete breathers in bcc metals V, Fe and W. *Comput. Mater. Sci.* **98**, 88–92 (2015)
20. O.V. Bachurina, Linear discrete breather in fcc metals. *Comput. Mater. Sci.* **160**, 217–221 (2019)
21. O.V. Bachurina, Plane and plane-radial discrete breathers in fcc metals. *Model Simul. Mater. Sci.* **27**(5), 055001 (2019)
22. P.V. Zakharov, E.A. Korznikova, S.V. Dmitriev, E.G. Ekomasov, K. Zhou, Surface discrete breathers in Pt₃Al intermetallic alloy. *Surf. Sci.* **679**, 1–5 (2019)
23. B. Eiermann, T. Anker, M. Albiez, M. Taglieber, P. Treutlein, K.P. Marzlin, M.K. Oberthaler, Bright Bose-Einstein gap solitons of atoms with repulsive interaction. *Phys. Rev. Lett.* **92**(23), 230401 (2004)
24. P. Binder, D. Abraimov, A.V. Ustinov, S. Flach, Y. Zolotaryuk, Observation of breathers in Josephson ladders. *Phys. Rev. Lett.* **84**(4), 745–748 (2000)
25. J.J. Mazo, T.P. Orlando, Discrete breathers in Josephson arrays. *Chaos* **13**(2), 733–743 (2003)
26. E. Trias, J.J. Mazo, T.P. Orlando, Discrete breathers in nonlinear lattices: experimental detection in a Josephson array. *Phys. Rev. Lett.* **84**(4), 741–744 (2000)
27. L.Q. English, F. Palmero, P. Candiani, J. Cuevas, R. Carretero-Gonzalez, P.G. Kevrekidis, A.J. Sievers, Generation of localized modes in an electrical lattice using subharmonic driving. *Phys. Rev. Lett.* **108**(8), 084101 (2012)
28. I.G. Bostrem, E.G. Ekomasov, J. Kishine, A.S. Ovchinnikov, V.E. Sinitsyn, Dark discrete breather modes in a monoaxial chiral helimagnet with easy-plane anisotropy. *Phys. Rev. B* **104**, 214420 (2021)
29. Y.S. Kivshar, M. Peyrard, Modulational instabilities in discrete lattices. *Phys. Rev. A* **46**(6), 3198–3205 (1992)

30. L. Kavitha, A. Muniyappan, A. Prabhu, S. Zdravkovic, S. Jayanthi, D. Gopi, Nano breathers and molecular dynamics simulations in hydrogen-bonded chains. *J. Biol. Phys.* **39**(1), 15–35 (2013)
31. A. Maluckov, L. Hadžievski, N. Lazarides, G.P. Tsironis, Extreme events in discrete nonlinear lattices. *Phys. Rev. E* **79**, 025601 (2009)
32. E.A. Korznikova, D.V. Bachurin, S.Y. Fomin, A.P. Chetverikov, S.V. Dmitriev, Instability of vibrational modes in hexagonal lattice. *Eur. Phys. J. B* **90**, 23 (2017)
33. O.V. Bachurina, A.A. Kudreyko, Two-dimensional discrete breathers in fcc metals. *Comput. Mater. Sci.* **182**, 109737 (2020)
34. O.V. Bachurina, A.A. Kudreyko, Two-component localized vibrational modes in fcc metals. *Eur. Phys. J. B* **94**(11), 218 (2021)
35. LAMMPS, <http://lammmps.sandia.gov>
36. G.J. Ackland, Theoretical-study of titanium surfaces and defects with a new many-body potential. *Philos. Mag. A* **66**(6), 917–932 (1992)
37. R.G. Hennig, T.J. Lenosky, D.R. Trinkle, S.P. Rudin, J.W. Wilkins, Classical potential describes martensitic phase transformations between the alpha, beta, and omega titanium phases. *Phys. Rev. B* **78**(5), 054121 (2008)
38. L.T. Kong, G. Bartels, C. Campana, C. Denniston, M.H. Muser, Implementation of Green's function molecular dynamics: an extension to LAMMPS. *Comput. Phys. Commun.* **180**(6), 1004–1010 (2009)
39. N.K. Voulgarakis, G. Hadjisavvas, P.C. Kelires, G.P. Tsironis, Computational investigation of intrinsic localization in crystalline Si. *Phys. Rev. B* **69**(11), 113201 (2004)
40. V. Hizhnyakov, M. Haas, M. Klopov, A. Shelkan, Discrete breathers above phonon spectrum. *Lett. Mater.* **6**(1), 61–72 (2016)
41. V. Hizhnyakov, M. Haas, A. Shelkan, M. Klopov, Standing and moving discrete breathers with frequencies above the phonon spectrum, in *Quodons in Mica*. (Springer, Berlin, 2015), pp. 229–245
42. J.H. Los, A. Fasolino, Intrinsic long-range bond-order potential for carbon: performance in Monte Carlo simulations of graphitization. *Phys. Rev. B* **68**(2), 024107 (2003)
43. V. Hizhnyakov, M. Haas, A. Shelkan, M. Klopov, Theory and molecular dynamics simulations of intrinsic localized modes and defect formation in solids. *Phys. Scripta* **89**(4), 044003 (2014)
44. R.T. Murzaev, A.S. Semenov, A.I. Potekaev, M.D. Starostenkov, P.V. Zakharov, V.V. Kulagina, S.V. Dmitriev, Spatially localized oscillations in low-stability states of metal systems. *Russ. Phys. J.* **64**(2), 293–301 (2021)
45. A. Upadhyaya, M.N. Semenova, A.A. Kudreyko, S.V. Dmitriev, Chaotic discrete breathers and their effect on macroscopic properties of triangular lattice. *Commun. Nonlinear Sci. Numer. Simul.* **112**, 106541 (2022)
46. M. Singh, A.Y. Morkina, E.A. Korznikova, V.I. Dubinko, D.A. Terentiev, D. Xiong, O.B. Naimark, V.A. Gani, S.V. Dmitriev, Effect of discrete breathers on the specific heat of a nonlinear chain. *J. Nonlinear Sci.* **31**(1), 1–27 (2021)